GAAS® 97 • 5th European Gallium Arsenide and related III-V compounds Applications Symposium
Bologna, Italy - September 3rd-5th, 1997

An improved C-V model of GaAs MESFETs for CAD of high speed circuits and broadband amplifiers

Agostino Giorgio, Anna Gina Perri

Dipartimento di Elettrotecnica ed Elettronica, Politecnico di Bari
Via E. Orabona 4, 70125, Bari, Italy
Phone: +39 - 80 - 5460427 -5460314 Fax: +39-80-5460410, E-mail: perri@poliba.it

Abstract - *In this paper a semiempirical capacitance model of GaAs FET, very useful for CAD of MMIC, is proposed. The model fits the results of two dimensional (2-D) simulations of device behaviour, accounting for the most important microwave effects, by means of the determination of an effective shape of the depletion region in the active channel.*
Simple physical equations and a few effective empirical parameters, with a precise physical meaning, are employed. So the initial estimation of parameters and their extraction procedure result to be very easy.
In spite of its semiempirical nature the model does not leave the control over physical and technological device parameters to circuit designer, necessary to achieve a reliable design.
The model usefulness and accuracy are experimentally confirmed to be very satisfactory for different kinds of MESFETs.

Introduction

A reliable design of high speed circuits and broadband amplifiers employing GaAs MESFETs requires more and more accurate internal device capacitance models, useful for CAD tools implementation.
Moreover, many physical effects significantly affect the dynamic behaviour of GaAs MESFETs and the internal capacitance variation with the bias voltages, making the development of enough accurate and at the same time quite simple capacitance models of the device very difficult [1-2].
Two modeling approaches are generally followed: the empirical and the physical one.
Empirical models [3-4] satisfy those requirements necessary for their implementation in computer programs but have at least two disadvantages. First of all, the designer loses direct control over physical and technological device parameters. This control is very important for a reliable, high yield, circuit design [5-6]. Secondly, the characterization procedure to extract empirical parameter values is generally a very hard work, especially because it is often very difficult to find optimal initial parameter values to input in the extraction routine [3-4].
Physical models are always very complicated if they must account for the main physical effects affecting the device dynamic behaviour. So models simplicity fights against accuracy; therefore adjustement empirical parameters are often used [7-8] assuming typical values, with a loss in accuracy with respect to empirical models. The crucial step is to examine accurate numerical 2-D simulations of potential and field distribution in the device channel. The numerical results must then be expressed in analytical form by model equations. This implies approximations that are not always satisfactory, or gives rise to very complicated equations. Besides, the complication significantly grows if the physical model is developed referring to ion implanted devices [9].
Hence the problems associated with C-V (Capacitance-Voltage) modeling for CAD of GaAs MESFETs are to develop quite simple and accurate equations for any kind of MESFET, as for empirical models, and to give to the MMIC designer control over physical and technological device parameters, as for physical models. Furthermore the C-V models must also require an easy characterization procedure if empirical parameters must be extracted.

The proposed C-V model

The internal GaAs MESFET capacitances (gate-source and gate-drain, C_{gs} and C_{gd} respectively) are defined as:

$$C_{gs} = \left.\frac{\partial Q_g}{\partial V_s}\right|_{V_{gd}=\text{cost}} \qquad C_{gd} = \left.\frac{\partial Q_g}{\partial V_d}\right|_{V_{gs}=\text{cost}} \tag{1}$$

where Q_g is the charge under the gate.
The shape of the depletion region in the active channel depends on many device features: the technology to fabricate the active channel (epitaxial or ion-implanted) [9], the occupied surface states in the gate-source and gate-drain interspace [5], backgating [10], capping [9], fringing effects and, obviously, polarization conditions.
For a uniformly doped channel and in velocity saturation condition, the space charge region is shown schematically in fig. 1, in which the linear region (I) and the saturation one (II-III) are distinguished [11-13].

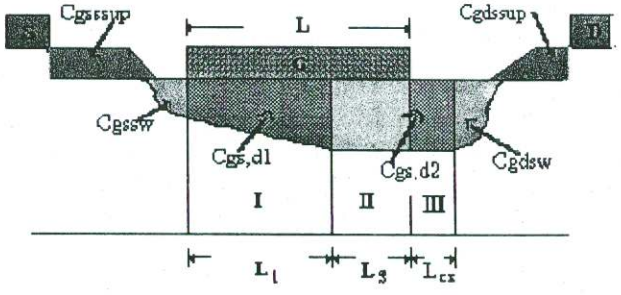

Fig.1 - Shape of the depletion region in the active channel of GaAs MESFET.

The two regions are defined by the condition in which the longitudinal electric field in the channel is respectively less or greater than the electron velocity saturation field. At the end of region III the field again becomes less than the saturation one [11].

Therefore it is useful to distinguish among contribution to capacitances due to fringing effects, accounted in the term $C_{gs,dsw}$ [9], surface states, accounted in $C_{gs,dssup}$ [5] and the contribution due to the space charge in the linear and saturation region, $C_{gs,d1}$ and $C_{gs,d2}$ respectively.

In this way the capacitances are expressed as follows:

$$C_{gs,d} = C_{gs,d1} + C_{gs,d2} + C_{gs,dssup} + C_{gs,dsw} \qquad (2)$$

where:

$$C_{gsssup} = qWL_{sg}D_{ds}; \qquad C_{gssw} = \frac{\pi \varepsilon \ W}{2}\left(1 - \frac{\partial V_{eps}}{\partial V_s}\right)$$

$$C_{gdssup} = qW_s N_D \frac{\partial\left(L_{gd} - L_{ex}\right)}{\partial V_d} + qW\left(L_{gd} - L_{ex}\right)D_{dgd}$$

$$C_{gdsw} = \varepsilon \, \mathrm{Warcsin}\sqrt{\frac{V(L_1, h(L_1))}{V(L_2, h(L_2))}}$$

$$L_2 = L_s + L_{ex}$$

being q the electron charge, L and W the device gate length and width respectively, N_D the uniform doping concentration, L_{sg} the gate-source spacing, L_{gd} the gate-drain spacing, $D_{ds} = \partial D_s/\partial V_s$ with D_s the surface state density, $W_s = D_s/N_D$ the thickness of the depletion region due to surface states, $D_{dgd} = \partial D_s/\partial V_d$; V_s and V_d the channel potential at source and drain edge of the gate; L_{ex} the extension of the depletion layer in the gate-drain interspace. Moreover h(x) is the depletion layer thickness, named h(S) and h(D) at the source and drain sections respectively; V(x,y) is the channel potential. V_{eps} and V_{epd} are the absolute values of the potential at the edge of the depletion region at the source and drain sections respectively and appear in h(S) and h(D) [11].

The determination of V_{eps} and V_{epd} and of their variation with bias voltages by analytical calculations is particularly complicated especially if it accounts for the diffusion of electrons and backgating [11]. Therefore, as it will be described later, it was made the numerical calculation of channel potential and then a polynomial approximation of the results, carried out automatically by a fast computer routine.

In fact, in order to calculate $C_{gs,d1}$ and $C_{gs,d2}$ in equation (2) a precise estimation of the shape of the depletion region, and therefore of the space charge, and of the potential distribution in the active channel by 2-D calculations, was carried out.

Moreover, to achieve a further improvement of the model accuracy, compensating approximations with which numerical results are modeled and the tolerances with which the technological device parameters are determined, a depletion region shape equivalent to the real one, as shown in fig. 2, was calculated introducing empirical parameters in the space charge region.

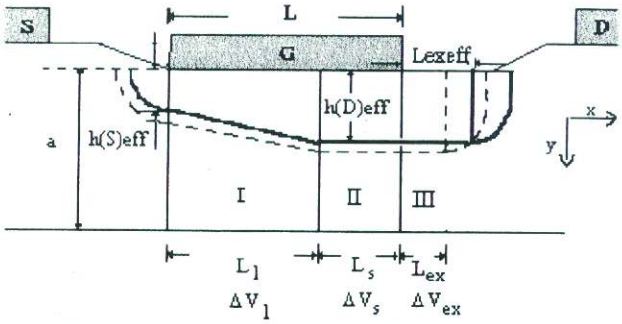

Fig.2 - The calculated (dashed) and the effective depletion region shape obtained with empirical parameters.

These parameters have a precise physical meaning and also allow to adapt the model to ion implanted devices. They are: the effective thickness of the depletion region beneath the drain and source end of the gate, the effective $\partial D_s/\partial V_s$, D_{dseff}, and the effective depletion region length in the gate-drain interspace. So the depletion region extensions and their variation with bias voltages are determined considering:

$$h(S)_{eff} = C_1 * h(S); \quad h(D)_{eff} = C_2 * h(D); \quad L_{exeff} = C_3 * L_{ex} \qquad (3)$$

in which C_i are empirical coefficients whose value is close to the unity.

Therefore, the physical meaning of effective parameters also allows an easy estimation of their initial values by approximated physical expressions [11] to start the extraction routine. The parameters are obtained one at a time minimizing the error between measured and modeled capacitance values for C_{gs} and for C_{gd} separately in linear and in electron velocity saturation region. In this way the characterization procedure is particularly simple and the parameter exctraction is remarkably stable.

Finally, in spite of the semiempirical nature of the proposed model, the control over physical and technological device parameters is still kept.

Therefore the charges Q_1 in the linear region and Q_2 in the saturation one are expressed as:

$$Q_1 = qWL_1 \int_0^{h(S)} N_D(y)dy + \frac{qWL_1}{h(D) - h(S)} \int_{h(S)}^{h(D)} N_D(y)\left[h(D) - y\right]dy$$

$$Q_2 = qWL_2 \int_0^{h(D)} N_D(y)dy$$

Making derivatives respect to bias voltages and using the effective parameters (3), the expressions used to calculate $C_{gs,d1}$ and $C_{gs,d2}$ are:

$$C_{gs,d1} = A\left[\left(h(D)_{eff} + h(S)_{eff}\right)\frac{\partial L_1}{\partial V_{s,d}} + L_1\left(\frac{\partial h(S)_{eff}}{\partial V_{s,d}} + \frac{\partial h(D)_{eff}}{\partial V_{s,d}}\right)\right]$$

$$C_{gs,d2} = 2A\left[h(D)_{eff}\frac{\partial L_{2eff}}{\partial V_{s,d}} + L_{2eff}\frac{\partial h(D)_{eff}}{\partial V_{s,d}}\right] \quad \text{with}$$

$A = 0.5qWN_D$ and $L_{2eff} = L_s + L_{exeff}$

In order to calculate the depletion layer thickness and extensions, h(D), h(S), L_{ex} in (3) and L_1, 2-D calculations

are considered accounting for backgating, electron diffusion, electron velocity saturation, surface states, Gunn domain formation and capping [11].
So the model allows to simulate the dependence of C_{gs} and C_{gd} on bias voltages and on the most important effects in microwave MESFET applications.
To determine the space charge profile under the gate in the linear region, extended up to L_1 in fig.2, it results always satisfactory to adopt the gradual channel approximation [14], to assume a weak variation of the potential in the channel length direction and then to solve the one-dimensional Poisson equation accounting for backgating and capping. In the saturation region it is necessary to solve the two dimensional Poisson equation in order to calculate the extension of the depletion region.
Then the channel potential was analytically modeled by third order polynomials.
Therefore, to calculate h(x) the channel potential is expressed as:

$$V(x,h(x)) = P_{1x}(V_{ds})*V_{gs}^3+P_{2x}(V_{ds})*V_{gs}^2+P_{3x}(V_{ds})*V_{gs}+P_{4x}(V_{ds}) \quad (4)$$

where P_{ix} (i=1-4) are polynomials varying with x and whose degree depends on the particular device, tipically being equal to 2.
Polynomial coefficients and degree are dependent on bias and technology, and are determined automatically by a fast computer routine that interpolates the 2-D determined potential values as polynomials.
Expressions close to (4) are calculated for V_{pes}, V_{ped} and for $V(L_1,h(L_1))$, $V(L_s,h(L_s))$ and $V(L_2,h(L_2))$ useful to calculate the depletion region extensions L_1, L_s and L_{ex} in (3) [11]. There are expressed from 2-D calculations as functions of the voltage drop across each of these regions (see fig. 2):

$$L_1 = F_1(\Delta V_1), \quad L_s = F_s(\Delta V_s), \quad L_{ex} = F_{ex}(\Delta V_{ex}) \quad (5)$$

Besides, recalling that $L_1 + L_s = L$ and $L_s + L_{ex} = L_2$, the depletion region extension is completely determined.
A very useful approximation for expressions (5) is in [11] and we do not recall them for the sake of the brevity. Anyway, to facilitate the calculation of derivatives respect to bias voltages, it is useful to express (5) in polynomial form, too.
In this way a very simple computation of the channel potential, of the depletion region thickness and extension and their variation with respect to bias voltages is obtained, that is necessary to determine the device capacitances.

Experimental results

To verify the accuracy of the proposed model and to compare it to the most accurate models already proposed in literature, S parameters were measured by the authors and then C-V curves were extracted for two kinds of MESFETs, 0.5x1200 μm^2 ion-implanted (MESFET 1) and 1x3600 μm^2 epitaxial channel (MESFET 2).

The extracted empirical parameter values are listed in table I.

	C_1	C_2	K_3	D_{dseff}
MESFET1	0.9510	0.9562	1.0490	1.050e15
MESFET2	0.9600	0.9561	1.0475	1.103e15

Table I.

where K_3 is the parameter of $(L_{gd}-L_{ex})_{eff}$, i.e. $C_3 = K_3 + (1-K_3)*L_{gd}/L_{ex}$.
The new model results the most accurate with a Mean Quadratic Error (M.Q.E.) of about 15.2e-29 F^2 for MESFET1 and of 14.7e-29 F^2 for MESFET2, compared to the modified version of Curtice model as implemented in PSPICE 4.2 [7] M.Q.E. 9e-27 F^2, and to the models developed respectively by Statz [8] M.Q.E. 4.5e-27 F^2, Ladbrooke [5] M.Q.E. 3.2e-26 F^2, Shur-Chen [9] M.Q.E. 6.0e-28 F^2, Rodriguez -Tellez [3] M.Q.E. 2.7e-27 F^2, Angelov [4] M.Q.E. 1.1e-27 F^2.
In figs. 3 and 4 measured (lines) and calculated with the new model (surfaces) capacitance values for both previuos devices, are superimposed.

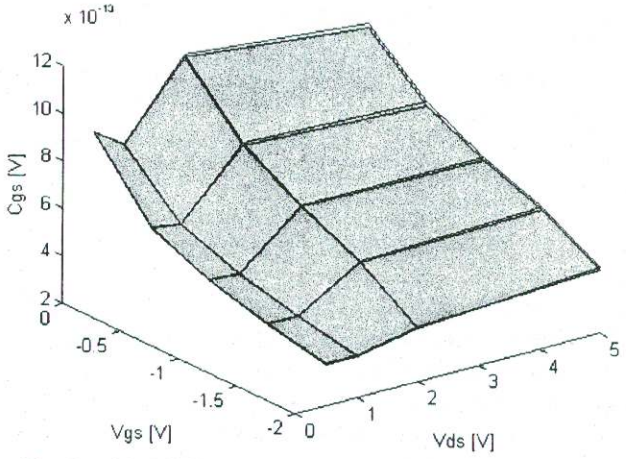

Fig. 3a - Modeled and measured C_{gs} values for MESFET1.

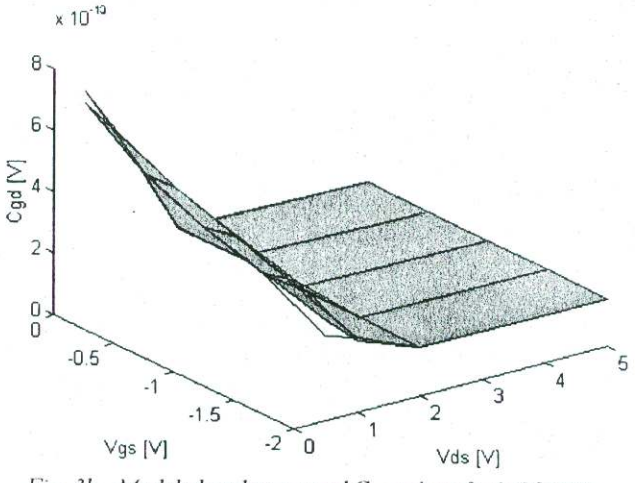

Fig. 3b - Modeled and measured C_{gd} values for MESFET1.

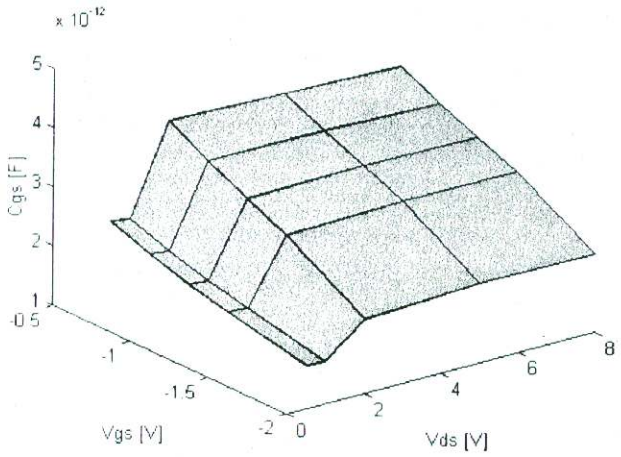

Fig. 4a - Modeled and measured C_{gs} values for MESFET2.

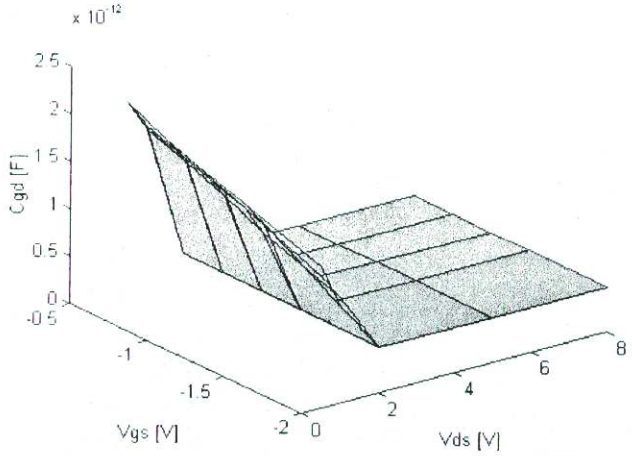

Fig. 4b - Modeled and measured C_{gd} values for MESFET2.

It is noticeable that for the epitaxial device (MESFET2) the error between measured and modeled values is pratically inappreciable. Anyway, also for the ion implanted device the model fits very well the measured values, to confirm the usefulness of empirical parameters to determine the equivalent space charge region extension and variation.

Conclusions

In this paper an improved model of internal capacitances of GaAs MESFET oriented to CAD tool implementation was proposed.

The model was based on semiempirical approach having the aim to improve approximations with which 2-D numerical calculations are analytically modeled by means of polynomials. Moreover, the physical meaning of the semiempirical parameters does not leave the control over physical and technological device parameters to circuit designer, necessary to achieve a reliable design.

Finally the semiempirical approach allows to adapt the proposed model to any kind of MESFETs.

Therefore, it was determined an effective space charge region profile, very close to the one determined from 2-D calculations, using only four empirical coefficients of the shape of the space charge region, easly extracted minimizing the error between measured and modeled capacitance values.

Furthermore, the model allows to simulate the dependence of C_{gs} and C_{gd} on bias voltages and on the most important effects in microwave MESFET applications. In fact, the 2-D calculations account for backgating, apparent channel pinch-off, electron velocity saturation, surface states, Gunn domain formation and capping.

References

[1] H. A. Willing, P. de Santis, "Modelling of Gunn-domain effects in GaAs MESFET's", Electronics Letters, vol.13, no. 18, September 1977.

[2] H. A. Willing, C. Rauscher, P. de Santis, "A technique for predicting large-signal performance of a GaAs MESFET", IEEE Trans. Microwave Theory Tech., vol. MTT-26, no.12, December 1978.

[3] J. Rodriguez-Tellez, K. Mezher, M. Al-Daas, "Improved junction capacitance model for the GaAs MESFET", IEEE Trans. Electron Devices, vol. ED-40, pp. 2083-2085, November 1993.

[4] I. Angelov, H. Zirath, N. Rorsman, "Validation of a nonlinear transistor model by power spectrum characteristics of HEMT's and MESFET's", IEEE Trans. Microwave Theory Tech., vol. MTT-43, no. 5, pp. 1046-1051, May 1995.

[5] P. H. Ladbrooke, S. R. Blight, "Low-field, low frequency dispersion of transconductance in GaAs MESFETs with implications for other rate-dependent anomalies", IEEE Trans. Electron Devices, vol. ED-35, pp. 258-267, March 1988.

[6] S. D'Agostino, A. Betti-Berutto, "Physics-based expressions for the nonlinear capacitances of the MESFET equivalent circuit", IEEE Trans. Microwave Theory Tech., vol. MTT-42, no.3, pp. 403-406, March 1994.

[7] W. R. Curtice, "A MESFET model for use in the design of GaAs integrated circuits", IEEE Trans. Microwave Theory Tech., vol. MTT-28, pp. 448-456, May 1980.

[8] H. Statz, P. Newman, I. W. Smith, R. A. Pucel, H. A. Haus, "GaAs FET device and circuit simulation in SPICE,", IEEE Trans. Electron Devices, vol. ED-34, pp. 160-169, February 1987.

[9] T. H. Chen, M. S. Shur, "Analytical models of Ion-Implanted GaAs FET's", IEEE Trans. Electron Devices, vol. ED-32, no.1, pp. 18-28, January 1985

[10] C. Kocot, C. A. Stolte, "Backgating in GaAs MESFET's", IEEE Trans. Electron Devices, Vol. ED-29, no.7, pp. 1059-1064, July 1982.

[11] A. Giorgio, A. G. Perri, "Modelli di capacità per grandi segnali di MESFET in GaAs: stato dell'arte e nuovi modelli più accurati", Internal Report no. 21/96/S, 1996.

[12] K. Yamaguchi, S. Asai, H. Kodera, "Two-Dimensional Numerical Anaalysis of stability Criteria of GaAs FET's", IEEE Tran. on Electron Devices, Vol. ED-23, no. 12, December 1976.

[13] M. Shur, "Analitycal models of GaAs FET's", IEEE Transactions on Electron Devices, Vol. ED-32, no.1, January 1985.

[14] R. Pucel, H.A. Haus, H. Statz, "Signal and noise properties of Gallium Arsenide Microwave Field-Effect Transistors", Advances in Electronics and Electron Physics, Academic Pree no. 38, pp. 195--266, 1975.